Achieving Complete Band Gaps of Water Waves with Shallow-Draft Cylinder Arrays

Jinyao Zeng, Xinyu Zhao, Xiaodong Sun, and Xinhua Hu*

Department of Materials Science and Key Laboratory of Micro- and Nano-Photonic Structures (Ministry of Education), Fudan University, Shanghai 200433, China

(Received 19 November 2022; revised 28 February 2023; accepted 29 March 2023; published 20 April 2023)

Conventionally, band gaps of water waves can be obtained with periodic arrays of bottom-mounted obstacles or vertical cylinders. However, such structures need to possess a large ratio of volume in water, and may not be easy to build and move in practical ocean engineering. Here, we theoretically propose and experimentally demonstrate that when the water surface is pierced by a fixed, rigid cylinder array, a complete band gap of water waves can be achieved, in which the propagation of water waves is forbidden in all the directions. Such a band gap can exist even when the cylinders have a draft much smaller than the water depth ($d \ll h$). Based on the complete band gap, a semicircular shape of the fixed-surface disk array is further constructed, which can block omnidirectional water waves generated by a point source.

DOI: 10.1103/PhysRevApplied.19.044058

I. INTRODUCTION

The interaction of waves with periodic structures is a key topic in wave physics [1–3]. Based on the Bloch theorem, the dispersion relationship of waves in periodic structures can be solved and expressed as band structures [1–3]. It is found that there can exist specific frequency or energy ranges called band gaps in which wave propagation is forbidden. Such effects of band gaps, first discovered for electron waves in a periodic potential field [4], are critical to understand various phenomena in solid-state physics and form the basis of modern electronic technology [2].

Unlike quantum electron waves, water waves are mechanical waves propagating in water, with the restoring force provided by gravity [5,6]. In recent years, there has been growing interest in studies of the propagation of water waves in three-dimensional (3D) periodic or near-periodic structures [7–36]. On one hand, water waves can be directly observed and thus used to demonstrate and understand subtle concepts or fascinating phenomena, such as Bloch waves [7–9], superlensing effect [19], focusing effect [20–24], effective negative gravity [25–28], cloaking effect [29–31], topological effects [32–34], and unidirectional transmission [35,36]. On the other hand, water waves can possess high power density and thus strongly influence human activities in oceans, including offshore drilling, offshore wind power, and aquaculture [6]. It is highly desired to construct appropriate structures to control the propagation of water waves [14–17]. Some periodic structures that possess band gaps of water waves have been discovered to block water waves [8–18,37–40]. Using particular geometric parameters, the band gap can even extend to the entire Brillouin zone, forming a complete band gap [9,11]. However, such structures are usually composed of bottom-mounted obstacles or vertical cylinders, which need to possess a large ratio of volume in water and may not be easy to build and move in practical ocean engineering.

In this paper, we theoretically propose and experimentally demonstrate that when the water surface is pierced by a fixed, rigid cylinder array, a complete band gap of water waves can be achieved, in which the propagation of water waves is forbidden in all the directions. Interestingly, such a complete band gap can still exist even when the cylinders have a draft much smaller than the water depth ($d \ll h$). Based on the complete band gap, omnidirectional water waves can be blocked by a semicircular shape of a fixed-surface disk array, which is verified by both experiments and simulations.

II. RESULTS

We consider linear, inviscid, and irrotational water waves in water pierced with a square lattice of fixed, vertical, circular, rigid cylinders, as shown in Figs. 1(a) and 1(b). The cylinders have a draft d, radius R, and period a. The water region without cylinders has a depth of h, and the water depth is $h - d$ under the cylinders. Set $\mathbf{r} = (x, y)$ in the horizontal plane and z as the vertical axis. $z = 0$ on the bottom, and $z = h$ on the free surface of water.

For harmonic water waves, a velocity potential $\Phi(x, y, z)e^{-i\omega t}$ can be introduced, so that $\nabla\Phi(x, y, z)e^{-i\omega t}$ is the velocity of water particle where $\nabla \equiv (\partial/\partial x, \partial/\partial y, \partial/\partial z)$, ω is angular frequency, and t is time. Φ satisfies the

*huxh@fudan.edu.cn

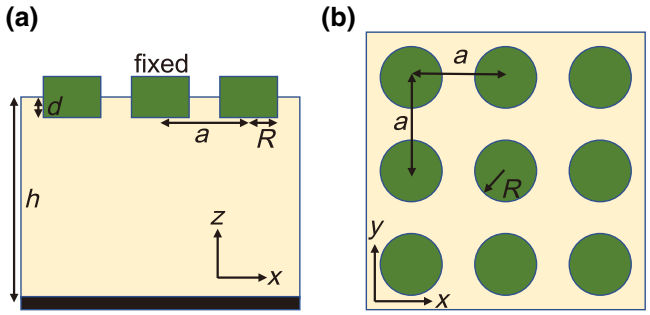

FIG. 1. Schematic diagrams of water pierced by a square lattice of fixed, vertical, rigid cylinders. The water depth is h. The cylinders have a period a, radius R, and draft d. (a),(b) Side and vertical views of the periodic system. The setup to fix the cylinders is not shown here.

3D Laplace's equation [5,6]

$$\nabla^2\Phi = 0 \tag{1}$$

subjected to boundary conditions

$$\frac{\partial\Phi}{\partial z} = 0 \text{ on } z = 0, \tag{2}$$

$$\frac{\partial\Phi}{\partial z} = \frac{\omega^2}{g}\Phi \text{ on } z = h, \tag{3}$$

$$\frac{\partial\Phi}{\partial \mathbf{n}} = 0 \text{ on the cylinder-water interface}, \tag{4}$$

where $\mathbf{n}$ is the unit vector normal to the cylinder-water interface.

If no cylinders exist in water, a solution of plane water waves exist for Eqs. (1)–(3), namely $\Phi = \exp(i\mathbf{k}\cdot\mathbf{r})\cosh(kz)/\cosh(kh)$ with $\mathbf{k} = (k_x, k_y)$ and $k = \sqrt{k_x^2 + k_y^2}$. From the dispersion

$$\omega^2 = gk\tanh(kh), \tag{5}$$

a real value of wave number k can be obtained for a given angular frequency ω [5,6]. In addition, many imaginary values of wave number k can also be obtained from Eq. (5), corresponding to evanescent waves.

When identical cylinders are arranged in the lattice, a solution of Bloch water waves exists for Eqs. (1)–(4), with the potential satisfying the Bloch condition

$$\Phi(\mathbf{r} + \mathbf{R}_{lm}, z) = \Phi(\mathbf{r}, z)\exp(i\mathbf{q}\cdot\mathbf{r}), \tag{6}$$

where $\mathbf{q} = (q_x, q_y)$ is the Bloch wave vector, $\mathbf{R}_{lm} = l\mathbf{a}_1 + m\mathbf{a}_2$ is the lattice vector, l and m are integers, $\mathbf{a}_1 = a\mathbf{e}_x$, $\mathbf{a}_2 = a\mathbf{e}_y$, and $\mathbf{e}_x$ and $\mathbf{e}_y$ are unit vectors in the x and y directions [1–3]. We adopt a commercial software (COMSOL Multiphysics) with the 3D finite-element method to simulate Eqs. (1)–(4) and (6). We consider a cuboid unit cell with a size of a in both the x and y directions and a height h in the z direction, and choose Bloch wave vectors $\mathbf{q}$ along the boundary of the first reduced Brillouin zone [see the inset to Fig. 2(a)]. For a given Bloch wave vector $\mathbf{q}$, multiple eigenfrequencies ω can be obtained. The results of $\omega(\mathbf{q})$ or $k(\mathbf{q})$ can then be plotted as band structures, where k is the wave number in water regions without cylinders.

It should be mentioned that when $d = h$, the structure in Fig. 1(a) will become a bottom-mounted cylinder array where Eqs. (1)–(4) and (6) reduce to a two-dimensional (2D) problem with $\Phi = \varphi(\mathbf{r})\cosh(kz)/\cosh(kh)$ [10–13, 19]. Hence, the band structures can be solved with the multiple scattering method [11], which can be used to check the accuracy of our 3D finite-element simulations.

Band structures of water waves are first calculated for the cases of $d \approx 0$ and $d = h$, as shown in Figs. 2(a) and 2(b). Here, the radius of cylinders $R = 0.4a$ and the water depth $h = 5a$. A complete band gap is visible between the first and second bands. The lower edge of the complete band gap is located at the M point of the first band, while the upper gap edge is situated at the X point of the second band. For the case of $d = h$ (i.e., a bottom-mounted cylinder array), the complete band gap has a wave number k ranging from 1.01 to $1.29\pi/a$. The 3D finite-element simulations can accurately reproduce the results by the rigorous multiple-scattering method [11], as shown in Fig. 2(b). For the case of $d \approx 0$ (i.e., a fixed-surface disk array), the complete band gap has a wave number k ranging from 1.55 to

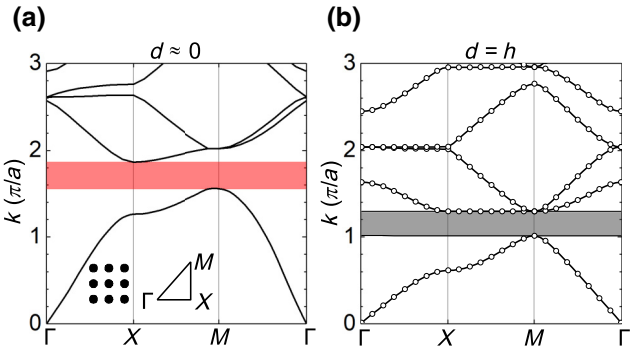

FIG. 2. Dispersion relationship of water waves in water pierced by a square lattice of fixed, vertical, rigid cylinders. The radius of cylinders $R = 0.4a$ and water depth $h = 5a$. (a) The draft of cylinders $d \approx 0$. (b) The cylinders are standing on the bottom ($d = h$). Circles are previous results [11] and solid lines denote our current results. The geometry of cylinders (top view) and the irreducible Brillouin zone are shown as the inset in (a). The red area in (a) and gray area in (b) denote the complete band gap.

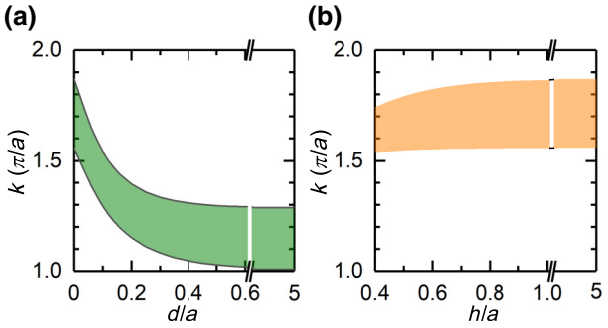

FIG. 3. The complete band gap as a function of (a) the draft of cylinders d or (b) the water depth h. $h = 5a$ and $R = 0.4a$ in (a). $d \approx 0$ and $R = 0.4a$ in (b).

$1.87\pi/a$, higher than the values in the case of $d = h$. A relative gap width $\Delta k/k$ can also be defined as the ratio of the gap width to the gap-center wave number. It is found that although the structure has a shallow draft ($d \ll h$), its relative gap width (18.3%) can still be 75% of the value (24.4%) of the structure of $d = h$.

Figure 3(a) shows the complete band gap as a function of the draft d of cylinders. Here, $R = 0.4a$ and $h = 5a$. We can see that when $d < 0.6a$, the wave numbers of the gap edges decrease with an increase in the draft d. However, when $d > 0.6a$, the gap will be almost independent of the draft d. Similar phenomena also appear in Fig. 3(b), which shows the gap as a function of water depth h. Here, $R = 0.4a$ and $d \approx 0$. It is found that when the water depth h is less than $0.6a$, the wave numbers k of the gap edges increase with increasing h. However, when $h > 0.6a$, the gap is basically independent of the water depth h. Such phenomena occur because water waves are surface waves with the potential decaying in the $-z$ direction ($\Phi \approx \Phi(z = h)\exp(-kz)$). For water waves in the gap, the potential is close to zero for $z < h - 0.6a$.

The position and width of the complete band gap also depend on the radius of cylinders R, as shown in Figs. 4(a) and 4(b). Here, the water depth $h = 5a$. We can see that when $0.5a > R > 0.32a$, increase of the radius of cylinders increases the gap width. However, if the radius of cylinders is less than the critical value ($R < 0.32a$), the complete band gap cannot exist. This explains why the complete band gap has not been discovered in previous studies, which dealt only with structures of $R \leqslant 0.05a$ [17]. Interestingly, the critical radius ($R_c = 0.32a$) for the occurrence of the complete band gap is independent of the water depth h and draft d. In addition, for the case of bottom-mounted cylinder arrays ($d = h$), the wave number of the lower gap edge (namely the upper boundary of the lowest band) decreases with an increase in the radius of cylinders R [Fig. 4(b)]. However, the opposite trend is found for the case of surface disk arrays ($d \ll h$). The difference reflects that in these two systems, water waves have different phase velocities in the lowest band, agreeing well with previous studies [20–22,35].

We conduct experiments to verify our theoretical results. Here, we adopt a vessel with a transparent bottom and slanted sides, so that no reflected waves will be generated at the boundaries. Water is placed in the vessel and then covered with a fixed rigid disk array with a semicircular shape, where the depth $h = 10$ cm and the draft of the disks $d = 1$ mm. [Fig. 5(a)]. The array consists of 45 rigid disks with $r = 8$ mm, $a = 20$ mm, and height of 8 mm, which is mounted on a rigid semicircular board and fabricated with polylactic acid (PLA) by means of 3D-printing technology [Fig. 5(b)]. A point source of water waves is placed on the left side of the array, and the amplitude of water waves is smaller than the draft of the disks. By using a projection apparatus, the wave patterns are displayed on the screen [Fig. 5(a)].

Figures 5(c) and 5(d) show measured wave patterns for the cases in the lowest band and the complete band gap, respectively. For a wavelength of 37 mm, the wave number ($k = 1.09\pi/a$) is located in the lowest band. Hence, water waves can propagate through the disk array and thus be observed on the right of the array [Fig. 5(c)]. In contrast, for wavelength of 25 mm, the wave number ($k = 1.6\pi/a$) is inside the complete band gap. Since water waves are blocked by the array, they are weak and thus difficult to observe on the right of the array [Fig. 5(d)]. We note that if the array contains more rigid disks, transmitted water waves will disappear completely. When a shorter wavelength (in the second passing band) is applied, transmitted water waves can occur on the right of the disk array [not shown].

We also perform 3D finite-element simulations for the experiments, as shown in Figs. 5(e) and 5(f). Good agreement can be seen between theoretical and experimental results. For the lowest band, the phase velocity of water waves in the array is larger than that in water regions without structures, so that a longer wavelength can be observed in the array [Fig. 5(e)]. For wavelengths inside

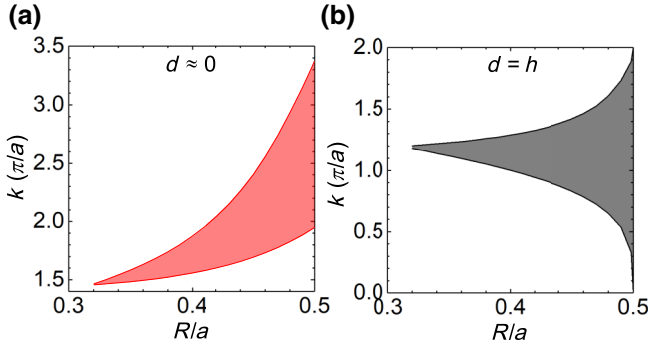

FIG. 4. The complete band gap as a function of the radius of cylinders R for structures with (a) $d \approx 0$ and (b) $d = h$. The water depth $h = 5a$.

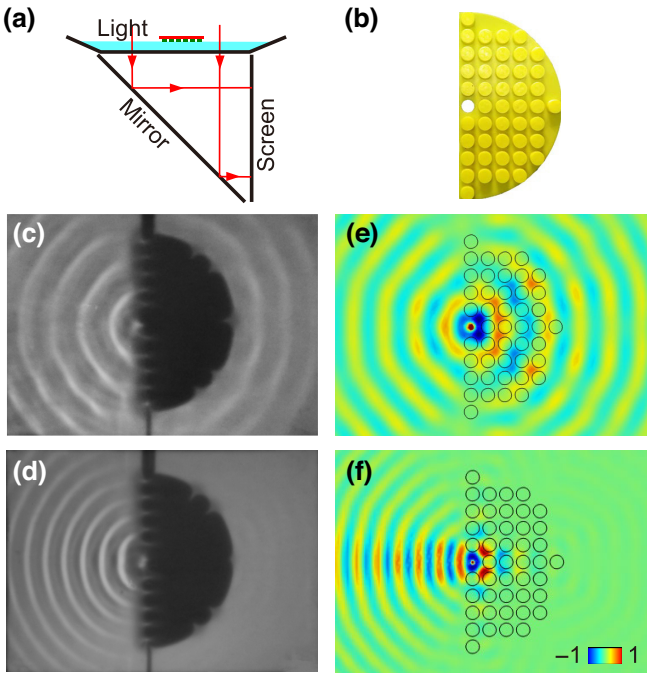

FIG. 5. Demonstration of the complete band gap of water waves in water covered by a fixed, rigid disk array. The array has a semicircular shape and a point source of water waves is placed on its left side. The parameters are $h = 10$ cm, $a = 20$ mm, $r = 8$ mm, and $d = 1$ mm. (a) Schematic diagram of the experimental setup. Water is placed in a vessel with a transparent bottom and slanted sides. Using a mirror and collimated light, the pattern of water waves can be projected onto a screen. (b) Photograph of the disk array consisting of 45 PLA disks mounted on a rigid board. (c),(d) Photographs of wave patterns. (e),(f) Simulated patterns of $\mathrm{Re}(\Phi)$ on the surface of water. In (c),(e), water waves have a wavelength of 37 mm and can pass through the disk array. In (d),(f), water waves have a wavelength of 24 mm and are blocked by the disk array.

the complete band gap, water waves are strongly reflected by the disk array. Therefore, a large amplitude of waves is discovered in the left central area of the array [Fig. 5(f)].

The above experiments verify that the complete band gap can indeed be realized by covering water with a fixed rigid disk array. Even when the disk array has a shallow draft ($d \ll h$), water waves can be completely blocked. We note that if water is only covered by a semicircular board without structures, internal waves (pressure waves) can exist under the board [41]. When the internal waves reach the edge of the board, they can be converted into surface waves in free water regions. As a result, transmitted waves can still be observed on the right side of the semicircular board (not shown).

III. SUMMARY

In summary, we theoretically and experimentally study the propagation of water waves in water with the surface pierced by a fixed, rigid cylinder array. We find that when the radius of cylinders exceeds a critical value ($R > 0.32a$), a complete band gap of water waves can exist even if the draft of cylinders is much smaller than the water depth ($d \ll h$). Via tuning the radius R and draft d of cylinders, both the width and position of the band gap can be flexibly adjusted. Based on the complete band gap, omnidirectional water waves, which are generated by a point source, can be blocked by a semicircular array of fixed-surface disks. The results provide an alternative mechanism to block water waves and should find applications in ocean engineering and coastal protection.

ACKNOWLEDGMENTS

This work is supported by the National Key Research and Development Program of China (2018YFA0306201) and NSFC (61422504 and 11574037).

[1] L. Brillouin, *Wave Propagation in Periodic Structures* (Dover, New York, 1953).
[2] N. W. Ashcroft and N. D. Mermin, *Solid State Physics* (Saunders College, Philadelphia, 1976).
[3] J. D. Joannoupoulos, R. D. Meade, and J. N. Winn, *Photonic Crystals* (Princeton University Press, New York, 1995).
[4] R. de L. Kronig and W. G. Penney, Quantum mechanics of electrons on crystal lattices, Proc. R. Soc. A: Math. Phys. Eng. Sci. **130**, 499 (1931).
[5] H. Lamb, *Hydrodynamics* (Cambridge University Press, Cambridge, England, 1995).
[6] C. C. Mei, *The Applied Dynamics of Ocean Surface Waves* (World Scientific, Singapore, 1989).
[7] M. Torres, J. P. Adrados, and F. R. M. de Espinosa, Visualization of Bloch waves and domain walls, Nature (London) **398**, 114 (1999).
[8] M. Torres, J. P. Adrados, F. R. M. de Espinosa, D. Garcia-Pablos, and J. Fayos, Parametric Bragg resonances in waves on a shallow fluid over a periodically drilled bottom, Phys. Rev. E **63**, 011204 (2000).
[9] X. Hu, Y. Shen, X. Liu, R. Fu, and J. Zi, Complete band gaps for liquid surface waves propagating over a periodically drilled bottom, Phys. Rev. E **68**, 066308 (2003).
[10] P. McIver, Water-wave propagation through an infinite array of cylindrical structures, J. Fluid Mech. **424**, 101 (2000).
[11] X. Hu, Y. Shen, X. Liu, R. Fu, J. Zi, X. Jiang, and S. Feng, Band structures and band gaps of surface waves propagating through an infinite array of cylinders, Phys. Rev. E **68**, 037301 (2003).
[12] T. S. Jeong, J. E. Kim, and H. Y. Park, Experimental measurement of water wave band gaps, Appl. Phys. Lett. **85**, 1645 (2004).
[13] H. Ge, B. Liang, and L. Zhang, Multi-frequency blocking effects by multiple vertical cylinders designed using combination grating theories, Ocean Eng. **265**, 112504 (2022).

[14] T. Chou, Band structure of surface flexural gravity waves along periodic interfaces, J. Fluid Mech. **369**, 333 (1998).
[15] G. Tokić and D. K. P. Yue, Hydrodynamics of periodic wave energy converter arrays, J. Fluid Mech. **862**, 34 (2009).
[16] L. G. Bennetts and V. A. Squire, Wave scattering by multiple rows of circular ice floes, J. Fluid Mech. **639**, 213 (2009).
[17] B. G. Carter and P. McIver, Water-wave propagation through an infinite array of floating structures, J. Eng. Math. **81**, 9 (2013).
[18] Y. Meng, Y. Hao, S. Guenneau, S. Wang, and J. Li, Willis coupling in water waves, New J. Phys. **23**, 073004 (2021).
[19] X. Hu, Y. Shen, X. Liu, R. Fu, and J. Zi, Superlensing effect in liquid surface waves, Phys. Rev. E **69**, 030201(R) (2004).
[20] X. Hu and C. T. Chan, Refraction of Water Waves by Periodic Cylinder Arrays, Phys. Rev. Lett. **95**, 154501 (2005).
[21] J. Yang, Y. F. Tang, C. F. Ouyang, X. H. Liu, X. Hu, and J. Zi, Observation of the focusing of liquid surface waves, Appl. Phys. Lett. **95**, 094106 (2009).
[22] Z. Wang, P. Zhang, X. Nie, and Y. Zhang, Focusing of liquid surface waves by gradient index lens, EPL **108**, 24003 (2014).
[23] C. Li, L. Xu, L. Zhu, S. Zou, Q. H. Liu, Z. Wang, and H. Chen, Concentrators for Water Waves, Phys. Rev. Lett. **121**, 104501 (2018).
[24] A. J. Archer, H. A. Wolgamot, J. Orszaghova, L. G. Bennetts, M. A. Peter, and R. V. Craster, Experimental realization of broadband control of water-wave-energy amplification in chirped arrays, Phys. Rev. Fluids **5**, 062801(R) (2020).
[25] X. Hu, C. T. Chan, K. M. Ho, and J. Zi, Negative Effective Gravity in Water Waves by Periodic Resonator Arrays, Phys. Rev. Lett. **106**, 174501 (2011).
[26] X. Hu, J. Yang, J. Zi, C. T. Chan, and K. M. Ho, Experimental observation of negative effective gravity in water waves, Sci. Rep. **3**, 1916 (2013).
[27] G. Dupont, F. Remy, O. Kimmoun, B. Molin, S. Guenneau, and S. Enoch, Type of dike using C-shaped vertical cylinders, Phys. Rev. B **96**, 180302(R) (2017).
[28] L. G. Bennetts, M. A. Peter, and R. V. Craster, Graded resonator arrays for spatial frequency separation and amplification of water waves, J. Fluid Mech. **854**, R4 (2018).
[29] M. Farhat, S. Enoch, S. Guenneau, and A. B. Movchan, Broadband Cylindrical Acoustic Cloak for Linear Surface Waves in a Fluid, Phys. Rev. Lett. **101**, 134501 (2008).
[30] S. Zou, Y. Xu, R. Zatianina, C. Li, X. Liang, L. Zhu, Y. Zhang, G. Liu, Q. H. Liu, H. Chen, and Z. Wang, Broadband Cloak for Water Waves, Phys. Rev. Lett. **123**, 074501 (2019).
[31] Y. Hua, C. Qian, H. Chen, and H. Wang, Experimental topology-optimized cloak for water waves, Mater. Today Phys. **27**, 100754 (2022).
[32] S. Wu, Y. Wu, and J. Mei, Topological helical edge states in water waves over a topographical bottom, New J. Phys. **20**, 023051 (2018).
[33] S. Wu and J. Mei, Double Dirac cones and zero-refractive-index media in water waves, EPL **123**, 59001 (2018).
[34] N. Laforge, V. Laude, F. Chollet, A. Khelif, M. Kadic, Y. Guo, and R. Fleury, Observation of topological gravity-capillary waves in a water wave crystal, New J. Phys. **21**, 083031 (2019).
[35] X. Zhao, X. Hu, and J. Zi, Fast Water Waves in Stationary Surface Disk Arrays, Phys. Rev. Lett. **127**, 254501 (2021).
[36] L. Han, S. Chen, and H. Chen, Water Wave Polaritons, Phys. Rev. Lett. **128**, 204501 (2022).
[37] A. D. Heathershaw, Seabed-wave resonance and sand-bar growth, Nature (London) **296**, 343 (1982).
[38] C. C. Mei, Resonant reflection of surface water waves by periodic sandbars, J. Fluid Mech. **152**, 315 (1985).
[39] Z. An and Z. Ye, Band gap and localization of water waves over one-dimensional topographical bottoms, Appl. Phys. Lett. **84**, 2952 (2004).
[40] H. W. Liu, Band gaps for Bloch waves over an infinite array of trapezoidal bars and triangular bars in shallow water, Ocean Eng. **130**, 72 (2017).
[41] F. Wang and H. Li, Pulse and pulsating supercharging phenomena in a semi-enclosed pipe, Sci. Rep. **13**, 1332 (2023).